A Novel Multimodal NIR-II Nanoprobe for Detection of Metastatic Lymph nodes and Targeting Chemo-Photothermal Therapy in Oral Squamous Cell Carcinoma

Yufeng Wang[1,2*], Wansu Zhang[3*], Pengfei Sun[3], Yu Cai[2], Wenguang Xu[1,2], Quli Fan[3#], Qingang Hu[1,2#], Wei Han [1,2#].

1. Department of Oral and Maxillofacial Surgery, Nanjing Stomatological Hospital, Medical School of Nanjing University, No 30 Zhongyang Road, Nanjing 210008, China.

2. Central Laboratory of Stomatology, Nanjing Stomatological Hospital, Medical School of Nanjing University, No 22 Hankou Road, Nanjing 210093, China.

3. Key Laboratory for Organic Electronics and Information Displays & Jiangsu Key Laboratory for Biosensors, Institute of Advanced Materials (IAM), Jiangsu National Synergetic Innovation Center for Advanced Materials (SICAM), Nanjing University of Posts & Telecommunications, No 9 Wenyuan Road, Nanjing 210023, China.

#Corresponding authors:

Wei Han, Department of Oral and Maxillofacial Surgery, Nanjing Stomatological Hospital, Medical School of Nanjing University, Nanjing, China. Phone: +86-025-83620140; Fax: +86-025-83620140; E-mail: doctorhanwei@hotmail.com;

Qingang Hu, Department of Oral and Maxillofacial Surgery, Nanjing Stomatological Hospital, Medical School of Nanjing University, Nanjing, China. Phone: +86-025-83620202; Fax: +86-025-83620202; E-mail: qghu@nju.edu.cn;

Quli Fan, Key Laboratory for Organic Electronics and Information Displays & Jiangsu Key Laboratory for Biosensors, Institute of Advanced Materials (IAM), Jiangsu National Synergetic Innovation Center for Advanced Materials (SICAM), Nanjing University of Posts & Telecommunications, Nanjing, China. Phone: +86-025-83620173; Fax: +86-025-83620173; E-mail: iamqlfan@njupt.edu.cn.

*These authors contributed equally to this work.

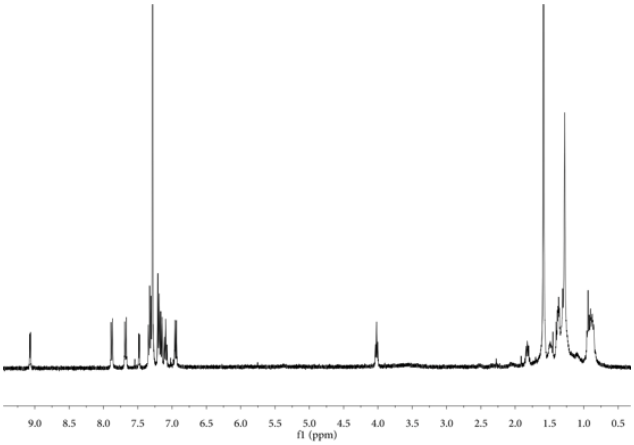

Figure S1 ^{1}H NMR (400 MHz, CDCl3) δ 9.07 (d, J = 4.1 Hz, 4H), 7.88 (d, J = 8.8 Hz, 9H), 7.68 (d, J = 8.7 Hz, 9H), 7.48 (d, J = 4.1 Hz, 5H), 7.40 – 7.26 (m, 67H), 7.13 (ddd, J = 36.5, 22.6, 14.6 Hz, 36H), 6.97 (t, J = 16.6 Hz, 12H), 4.02 (t, J = 6.5 Hz, 10H), 1.91 – 1.78 (m, 12H), 1.58 (s, 107H), 1.51 – 1.11 (m, 118H), 0.91 (dd, J = 16.1, 9.0 Hz, 39H)

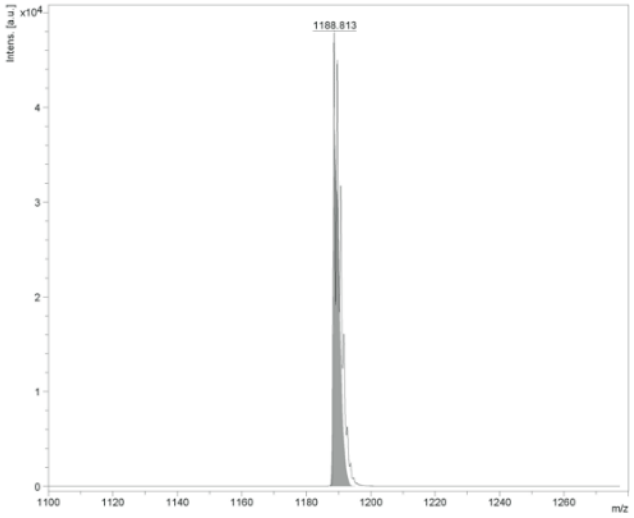

Figure S2 MALDI-TOF of TQTPA. The matrix-assisted laser desorption ionization time-of-flight mass spectroscopy (MALDI-TOF MS) measurements were carried out with a Shimadzu AXIMA-CFR mass spectrometer.

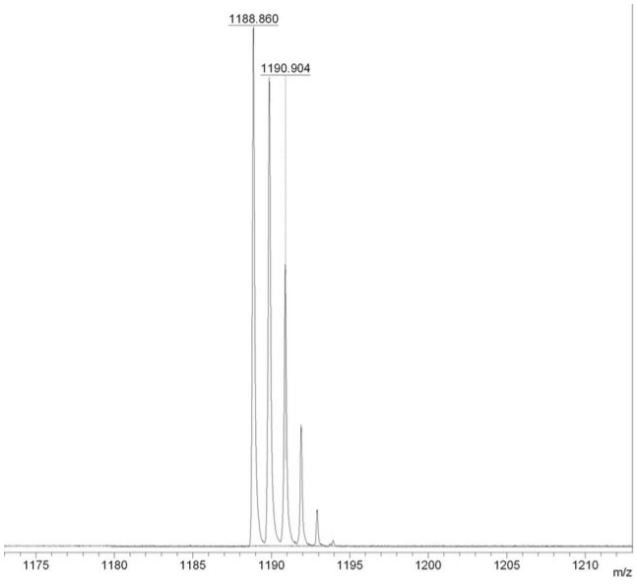

Figure S3 High resolution mass spectrometry of TQTPA.

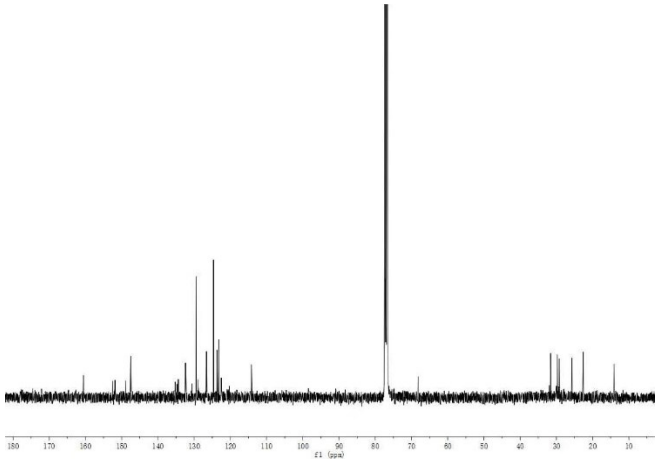

Figure S4 13C NMR of TQTPA.

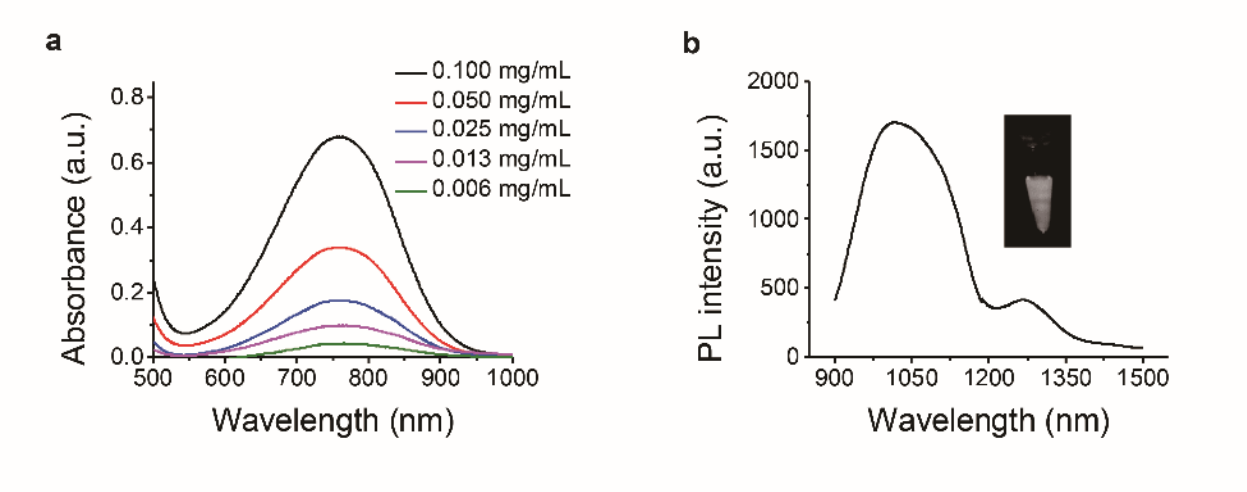

Figure S5 Characterization of TQTPA. (a) Ultraviolet-visible NIR spectra of TQTPA in tetrahydrofuran (THF) at different concentrations. (b) Fluorescence emission spectrum of TQTPA in THF. The concentration of TQTPA was 0.02 mg mL^{-1} and the power density was 40 mW cm^{-2}.

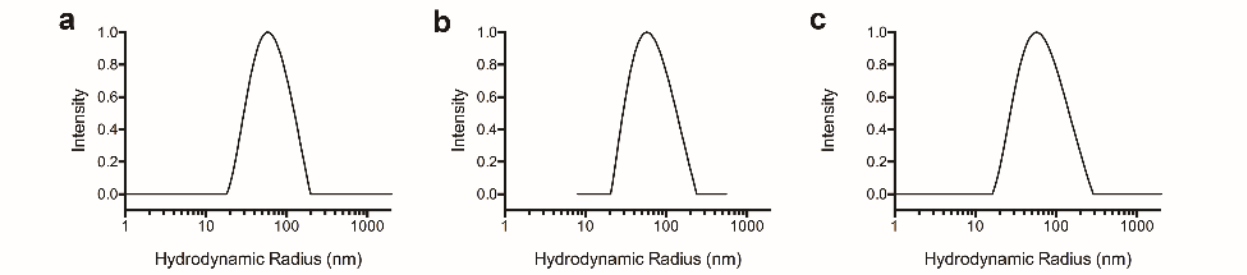

Figure S6 The hydrodynamic radius (Rh) of HT@CDDP NPs in PBS (a), DMEM (b) and FBS (c) determined by dynamic light scattering (DLS)

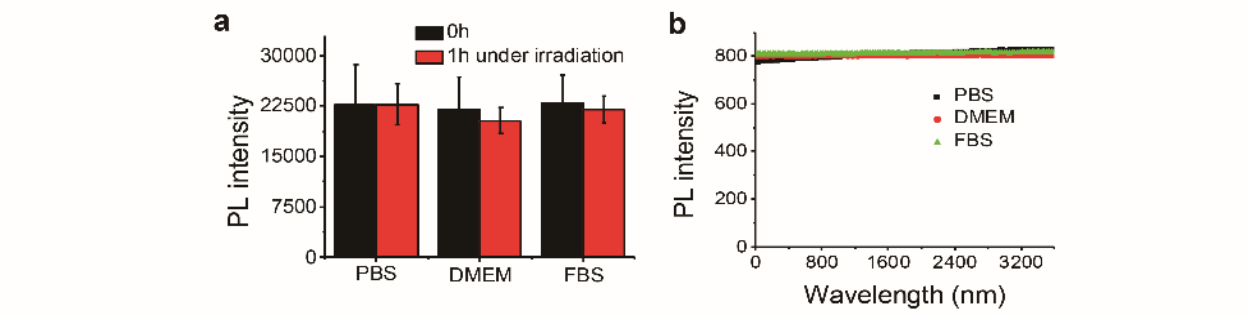

Figure S7 HT@CDDP NPs exhibited high photostability. The NPs were diluted in different medium and were irradiated for 1h. The PL intensity showed no obvious change in these three mediums.

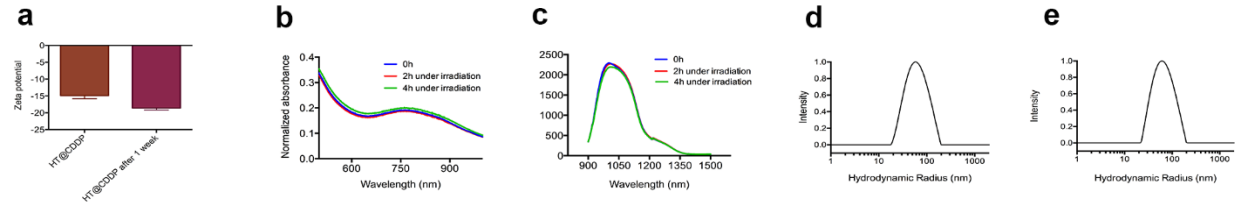

Figure S8 The stability of HT@CDDP NPs. a) Zeta potential measurement. Results are presented as mean ± SEM (n = 3). b) The absorbance of NPs after irradiation for 2h and 4 h. c) The emission spectra of NPs after irradiation for 2 h and 4 h. d) The DLS result of NPs in PBS at first day. e) The DLS result of NPs in PBS after a week.

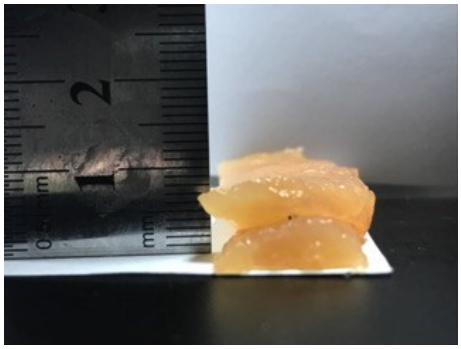

Figure S9 The model pattern for examination of the detection depth of NPs. A tiny tube filled with NPs solution was covered with chicken breasts tissue of different thicknesses. And we put them under NIR-II imaging system to see the NIR-II intensity.

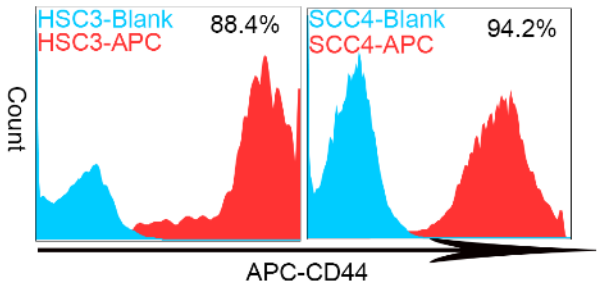

Figure S10 The ratios of CD44-positive cells in HSC3 and SCC4, as detected by flow cytometry.

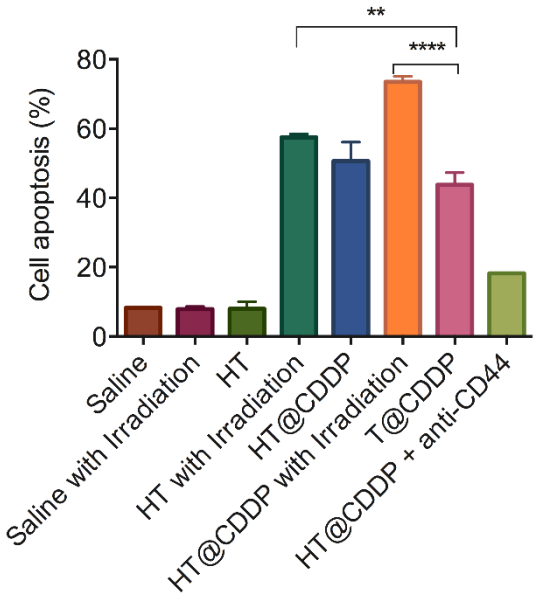

Figure S11 The quantified analysis of the ratio of apoptotic cells of HSC3 treated with different medium detected by Annexin V-FITC/PI staining kit and flow cytometry

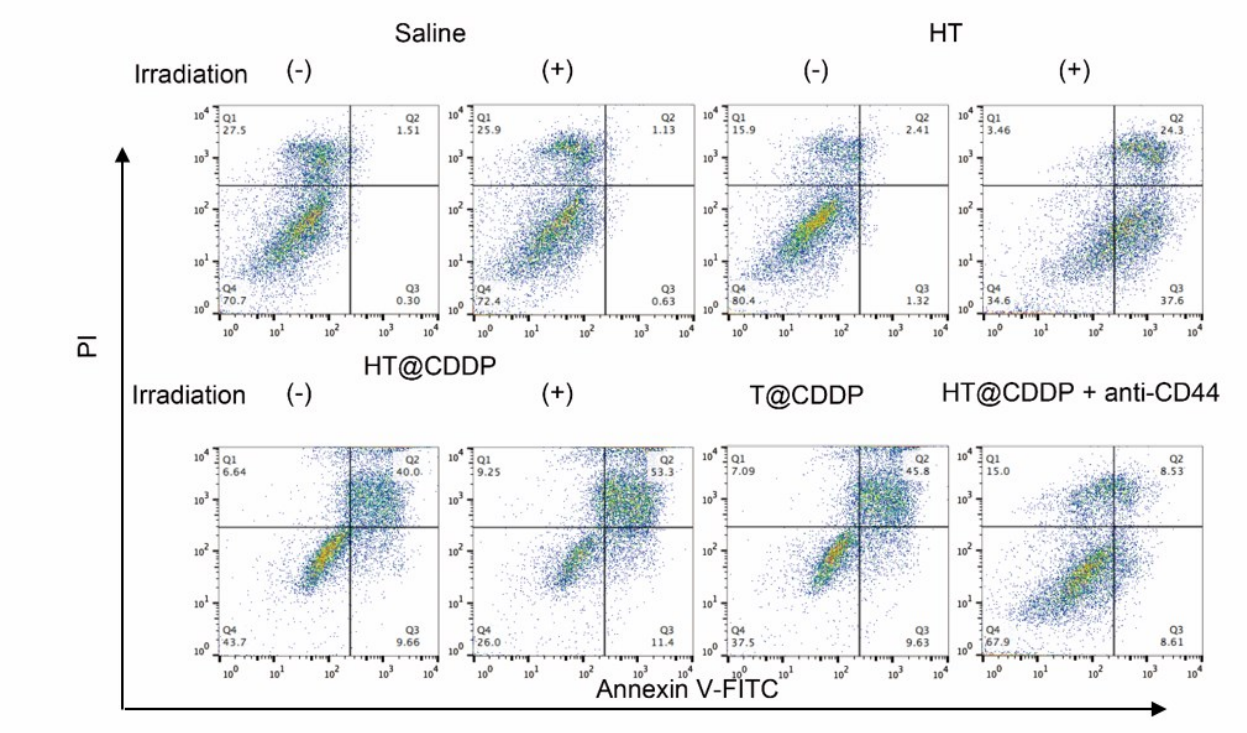

Figure S12 Cell apoptosis of SCC4 cells treated with different medium and examined by Annexin V-FITC/PI staining kit and flow cytometry.

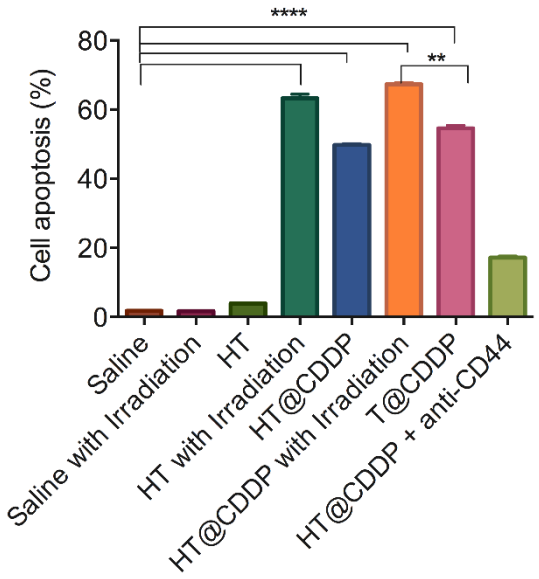

Figure S13 The quantified analysis of the ratio of apoptotic cells of SCC4 treated with different medium detected by Annexin V-FITC/PI staining kit and flow cytometry.

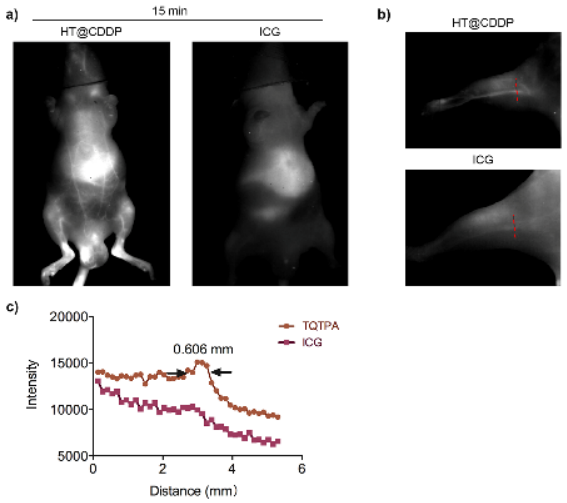

Figure S14 In vivo fluorescence images of HT@CDDP NPs (NIR-II) and ICG (NIR-I). (a) HT@CDDP NPs and ICG were injected intravenously into nude mice, and NIR images were obtained 15 min after injection. (b) Enlarged right femoral arteries. (c) Intensity analysis of red lines in (b).

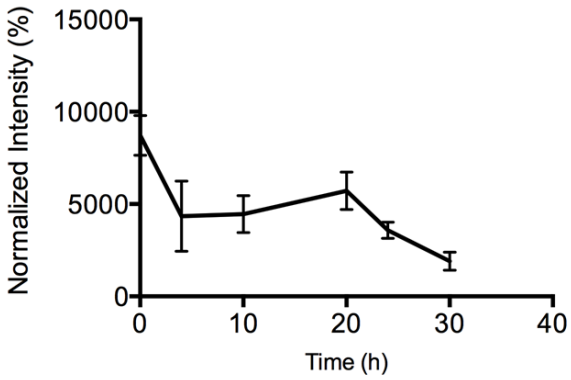

Figure S15 The signal intensity to background ratio (SBR) of ICG NIR-I imaging of orthotopic models. The results were presented as mean ± SD (n = 3).

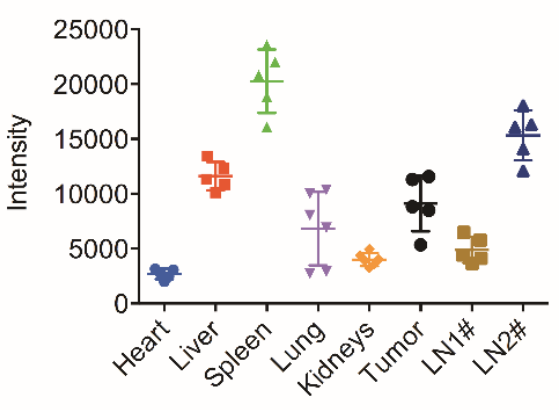

Figure S16 The NIR-II signal intensity of dissected organs, tumor and lymph nodes.

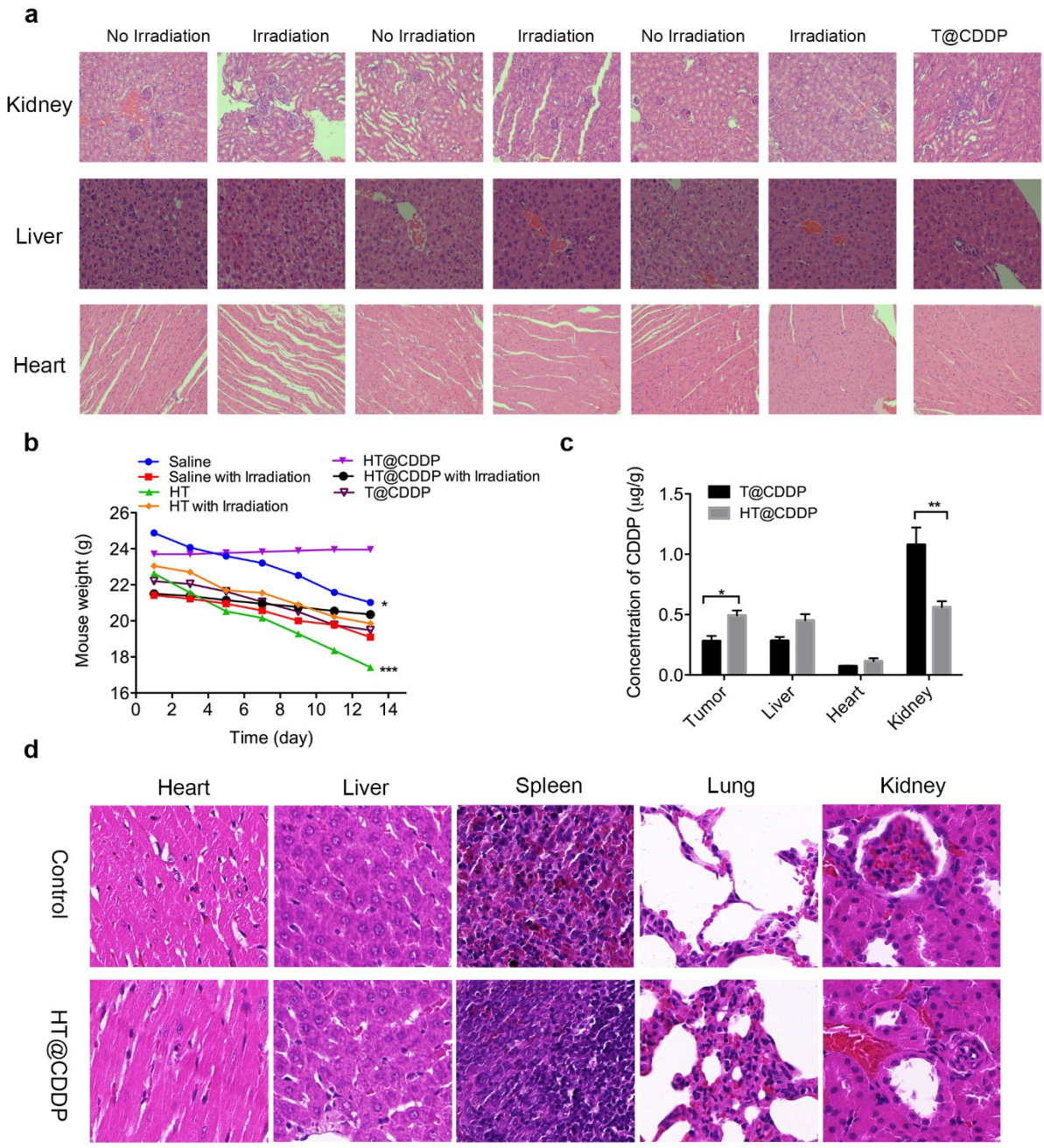

Figure S17 The biocompatibility of HT@CDDP. (a) HE staining of hearts, livers, and kidneys, demonstrating little damage to normal organs. (b) Mice weight curves. (c) CDDP concentration in the T@CDDP group and HT@CDDP group 7 days after tail vein injection. (d) HE staining of rat organs after 6 weeks.

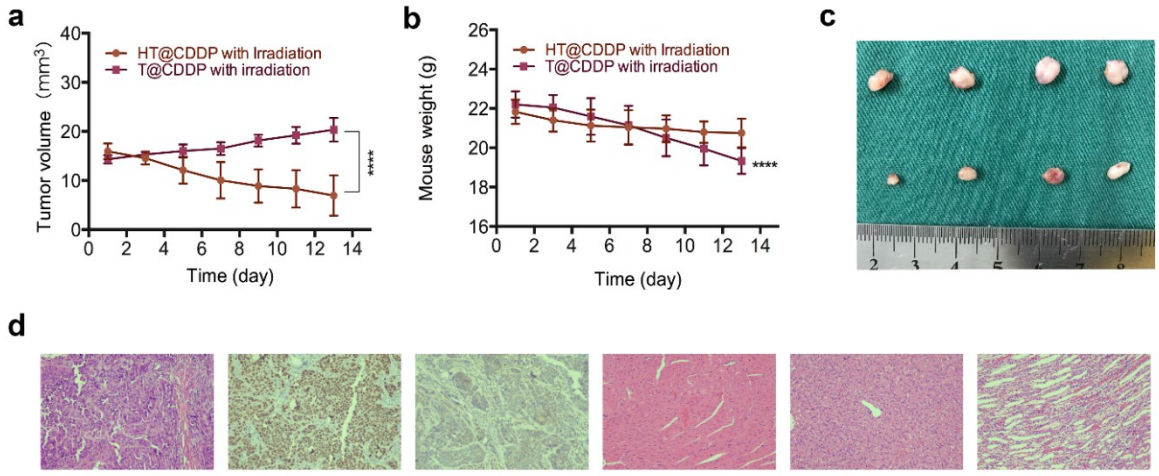

Figure S18 In vivo anti-tumor effect is detected by tumor sizes and results are expressed as the mean ± SEM (n = 4), *P < 0.05, **P < 0.01. a) Tumor volume curves. (b) Mice weight curves. (c) Mice tumor photographs; upper lane: T@CDDP with irradiation; lower lane: HT@CDDP with irradiation. d) From left to right: HE, Ki67, Bcl2 staining of tumor, HE staining of heart, liver, and kidney of group T@CDDP with irradiation.

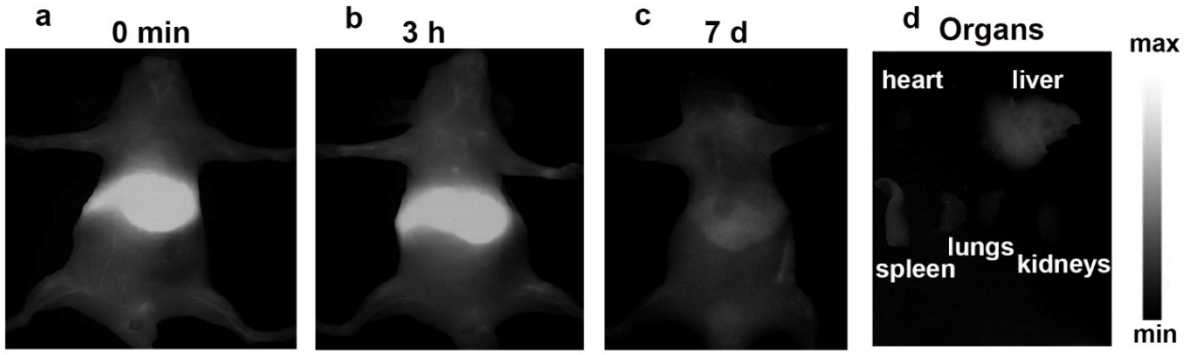

Figure S19 In vivo fluorescence images of nude mice after intravenous injection of HT@CDDP NPs. NIR images were obtained (a) immediately, (b) 3 hours, (c) 7 days after injection. (d) The NIR-II image of dissected organs after 7 days.

Table S1. Changes in BUN, Cr, and plasma enzyme levels after HT @CDDP treatment

	2 weeks	4 weeks	Reference Values
BUN	5.7	6.3	7.02~13.8 [mmol L^{-1}]
Cr	22	21	45.8~75.4 [μmol L^{-1}]
AST	131.4	164.2	60.8~154.7[U L^{-1}]
ALT	67.6	69.3	12.8~61.4 [U L^{-1}]